Taylor & Francis
Taylor & Francis Group

THE INFLUENCE OF SILANE COUPLING AGENT COMPOSITION ON THE SURFACE CHARACTERIZATION OF FIBER AND ON FIBER-MATRIX INTERFACIAL SHEAR STRENGTH

E. Feresenbet
D. Raghavan
Howard University, Chemistry Department, Washington, D.C., USA

G. A. Holmes
National Institute of Standards & Technology, Gaithersburg, Maryland, USA

It is well known that the fiber-matrix interface in many composites has a profound influence on composite performance. The objective of this study is to understand the influence of composition and concentration of coupling agent on interface strength by coating E-glass fibers with solutions containing a mixture of hydrolyzed propyl trimethoxysilane (PTMS) and γ-aminopropyl trimethoxysilane (APS). The failure behavior and strength of the fiber-matrix interface were assessed by the single-fiber fragmentation test (SFFT), while the structure of silane coupling agent was studied in terms of its thickness by ellipsometry, its morphology by atomic force microscopy, its chemical composition by diffuse reflectance infrared Fourier transform (DRIFT), and its wettability by contact angle measurement. Deposition of 4.5×10^{-3} mol/L solution of coupling agent in water resulted in a heterogeneous surface with irregular morphology. The SFFT results suggest that the amount of adhesion between the glass fiber and epoxy is dependent not only on the type of coupling agent but also on the composition of the coupling agent mixture. As the concentration of APS in the mixture increased, the extent of interfacial bonding between the fiber and matrix increased and the mode of failure changed. For the APS coated glass epoxy system, matrix cracks were formed perpendicular to the fiber axis in addition to a sheath of debonded interface region along the fiber axis.

INTRODUCTION

The demand for fiber-reinforced polymeric composites in aircraft, automobiles, ships, and housing is increasing. Approximately 95% of composites used today are fabricated from glass fibers, with epoxy resin being the preferred polymeric matrix because of the relatively good price-to-performance ratio, high availability, ease of processing, and dimensional stability. One of the major technical challenges to the use of composites in structural applications is the reliable prediction of long-term performance (*e.g.*, failure behavior, fatigue behavior, durability, stiffness). When composites are manufactured, a small region ($< 1\,\mu m$) known as the fiber-matrix interphase forms between the fiber and the matrix [1]. This region exhibits properties distinguishably different from the properties of the bulk matrix [2]. Since the fiber-matrix interphase transfers stress between the fiber and matrix, the efficiency of this stress-transfer process and a composite's strength and durability are controlled by this region's properties. The interphase stiffness, fiber topography, and fiber-matrix chemical bonding are critically important to the stress-transfer process and composite performance. The efficiency of this process is determined indirectly by micromechanics tests and quantified by a value termed the fiber-matrix interfacial shear strength (IFSS). In addition, micro-mechanics tests are used to probe a composite's strength, durability, and failure behavior.

A composite's interfacial performance is often improved by pretreating the fiber with adhesion promoters prior to manufacture [3]. In addition to protecting the fiber, these promoters are inexpensive, easy to apply, and have been observed to increase the bond strength at the interphase. Hence, the cost-to-performance ratio for using this material is very low. The strength and durability of the interface depends on the silane coupling agent's organo-functionality, concentration on the fiber, and the manner in which the silane-coated surface perturbs the curing reactions in the interphase region. Other factors that can affect interface strength and durability are the hydrolysis conditions during a silane coupling agent's deposition, the deposited silane layer morphology, and matrix-coupling agent compatibility (*i.e.*, wettability) [4, 5].

In 1975, Ahagon and Gent [6] explored the effect of covalent bonding on interface adhesion. This was accomplished by measuring the change in peel strength between a polybutadiene elastomer and glass plate coated with mixtures of bonding (vinyl trimethoxysilane) and nonbonding (ethyl trimethoxysilane) silane coupling agents. In 1996, Hunston *et al.* [7] used a similar approach to vary the degree of interfacial bonding between glass fibers and an epoxy matrix. In this research, mixtures of nonbonding (n-octadecyl trichlorosilane, OTS)

and bonding (γ-aminopropyl trimethoxysilane, APS) were coated on the fiber surface. Interfacial shear strength (IFSS) was determined by single fiber fragmentation tests (SFFTs) before and after water exposure. In both cases the interface strength increased as the concentration of reactive coupling agent increased. Since the chain length of the coupling agents were dissimilar, shielding of the APS group by the OTS could have reduced the accessibility of bonding sites. In this paper, bonding (APS) and nonbonding (PTMS) silane coupling agents of similar chain lengths were mixed in varying proportion to change systematically the degree of bonding (as measured by interfacial shear strength tests) between the glass fiber and epoxy matrix. Therefore, this research extends the research direction of Hunston *et al.* [7] by investigating, as in the Ahagon and Gent [6] research, the influence of equal chain length bonding and nonbonding coupling agents on fiber-matrix IFSS.

The properties of the deposited silane layer were investigated by ellipsometry (thickness), atomic force microscopy (morphology), Fourier transform infrared spectroscopy (chemical composition), and contact angle measurements (wettability). In this work, the fiber-matrix interfacial shear strengths of these model composites are measured by the SFFT. The SFFT is also used to draw inferences about the relationship between failure behavior and interface strength.

In the SFFT, a tensile load is applied to a dogbone specimen having a single fiber placed along the central axis. Since the fiber has a lower strain-to-failure than the resin, the fiber breaks at its weakest flaw as the strain increases. The fragmentation process continues until the remaining fiber fragments are all less than a critical transfer length (l_c). At this point, the fragmentation process has reached saturation. The critical transfer length is the length below which the fragments are too short for sufficient loads to transfer into them to cause failure. Once saturation has been reached, the specimen is allowed to relax back to the unstressed state, the fragment lengths are measured, and a micromechanics model is used to estimate the interfacial shear strength. Holmes *et al.* [8] have shown that when the E-glass fiber fragments during the test, the matrix exhibits nonlinear viscoelastic behavior. To account for this nonlinear viscoelastic matrix behavior in determining the fiber-matrix interfacial shear strength, a nonlinear viscoelastic shear-lag model was developed by Holmes *et al.* [8]. The equations for this model are as follows:

$$\tau_{\text{interface}} = \frac{d_f \beta\{\varepsilon, t\}}{4} \left(\frac{\sinh(\beta\{\varepsilon, t\} l_c/2)}{\cosh(\beta\{\varepsilon, t\} l_c/2) - 1} \right) \sigma_f\{l_c\},$$

where

$$\beta\{\varepsilon, t\} = \frac{2}{d_f}\left[\frac{E_m\{\varepsilon, t\}}{(1 + v_m)(E_f - E_m\{\varepsilon, t\})\ln(2r_m/d_f)}\right]^{1/2};$$

E_m, E_f are the matrix and fiber moduli, respectively; v_m is the matrix Poisson's ratio; ε is the global applied strain; t is the time; d_f is the fiber diameter; r_m is the radius of matrix parameter; l_c is the critical transfer length at saturation; and $\sigma_f\{l_c\}$ is the strength of the fiber at l_c.

EXPERIMENTAL[1]

Materials

γ-aminopropyl trimethoxysilane (APS, NH_2-CH_2-CH_2-CH_2-$Si(OCH_3)_3$) and propyl trimethoxysilane (PTMS, CH_3-CH_2-CH_2-$Si(OCH_3)_3$) were purchased from GELEST, INC. (Morrisville, PA, USA) and 2.0 mol/L hydrochloric acid (HCl) was purchased from Fisher Scientific (Suwanee, GA, USA). E-glass fibers, $15 \pm 3\,\mu m$ diameter, (from Owens Corning, Toledo, OH, USA), Epon 828 (Shell Chemical, Houston, TX, USA), and meta-phenylenediamine (m-PDA) (Fluka Chemical, Ronkonkama, NY, USA) were also used. All reagents were used without further purification.

Sample Preparation and Testing

Deposition of Coupling Agent on Glass Fiber

A 30 cm long tow was cut from a spool of E-glass fibers (specially prepared by Owens-Corning) previously shown to be free of processing aids by X-ray photoelectron spectroscopy (XPS) [9]. The tow was washed with spectrophotometeric grade acetone, vacuum dried at 110°C for 2 h, and cooled prior to use. Master batch solutions of 4.5×10^{-3} mol/L total silane were prepared for APS, PTMS, and APS/PTMS mixtures. 2.0 mol/L HCl was added using micropipette to each master batch solution to attain pH 4. A digital pH meter (PHH 320 Omega Engineering Inc., Stanford, CT, USA) with a standard glass electrode was used to determine the pH values. The silane solution was stirred for 1 h at room temperature. The coupling agent

---

[1] Certain commercial instruments and supplies are identified in this paper to adequately describe the experimental procedure. In no case does such identification imply recommendation or endorsement by the National Institute of Standards and Technology and Howard University, nor does it imply that instruments and supplies are the best available for this purpose.

was then coated on clean E-glass fibers by dipping the fiber tow in the silane mixture for 2 min. The tow was removed and allowed to air dry overnight at room temperature, followed by drying for 1 h at 110°C at −20 kPa in the vacuum oven. The coated fiber was cooled prior to use. Cleaning procedures, as well as coupling agent deposition process on the glass plate (Fisher Scientific, premium cover glass) and silicon wafers (⟨111⟩,Wacker Silitronic Corp., Portland, OR, USA) were conducted similar to the glass fibers.

Preparation of SFFT Specimens

The molds for preparing SFFT specimens were made with silicone rubber (RTV-664, General Electric, Waterford, NY, USA) following the procedure described by Drzal and Herrera-Franco [10]. All molds were postcured at 150°C and rinsed with acetone prior to use. Single filaments of coated E-glass fiber were carefully separated from the 30 cm tow. The individual fibers were aligned in the mold cavity *via* the sprue slots in the center of each cavity. The fibers were temporarily fixed in place by pressing them onto double-stick tape. Small strips of double-stick tape were placed over each fiber end to hold them in place until each fiber was permanently mounted with 5-min epoxy.

The SFFT specimens were prepared with a diglycidyl ether of bisphenol-A (DGEBA) epoxy, Epon 828 (Shell), cured using meta-phenylenediamine (m-PDA) (Fluka Chemical). One hundred grams of DGEBA and 14.5 grams of m-PDA were weighed out in separate beakers. To lower the viscosity of the resin and melt the m-PDA crystals, both beakers were placed in a vacuum oven set at 65°C. After the m-PDA crystals were completely melted, the silicone molds containing the fibers were placed into another vacuum oven that was preheated to 75°C at −20 kPa for 20 min. This last procedure dries the mold and minimizes the formation of air bubbles during the curing process. At approximately 9 min before the preheated molds were removed from the oven, the m-PDA is poured into the DGEBA and mixed thoroughly. The mixture was placed into the vacuum oven and degassed for approximately 7 min. After 20 min, the preheated molds were removed from the oven and filled with the DGEBA/m-PDA resin mixture using 10 ml disposable syringes. The filled molds were then placed into a programmable oven. A cure cycle of 2 h at 75°C followed by 2 h at 125°C was used.

Fragmentation Test

The fiber fragmentation tests were conducted in a manner similar to that described by Holmes *et al.* [8]. All specimens were tested with a 10 min delay between strain increments.
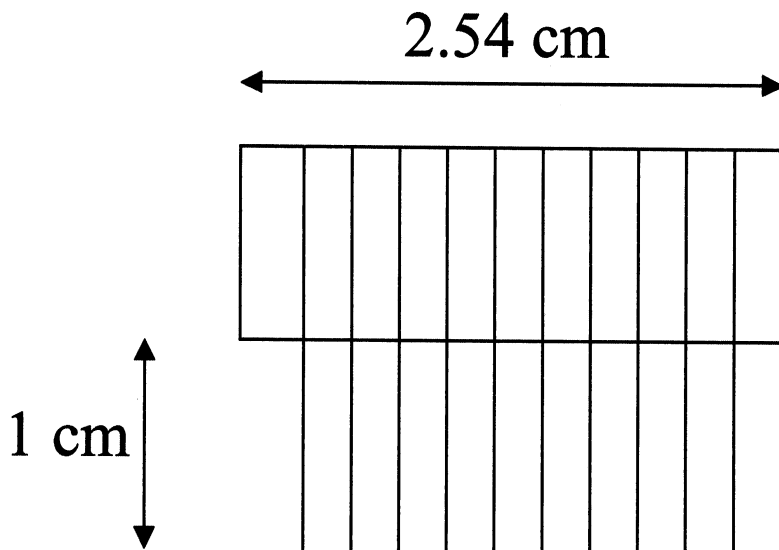
Characterization of Deposited Silane Layers

Tapping Mode Atomic Force Microscopy (TMAFM)

TMAFM was performed with a Dimension 3100 (Digital Instruments, West Grove, PA, USA) scanning probe microscope. Topographic images of coupling agents deposited on silicon wafers were recorded at ambient conditions. Commercial silicon cantilever probes, each with a nominal tip radius of 5 nm to 10 nm and spring constant in the range of 20 N/m (values provided by manufacturer) were oscillated at their fundamental resonance frequencies, which ranged between 250 kHz and 350 kHz. All TMAFM images were recorded using a free-oscillation amplitude of (60 ± 2) nm. Sequential scans gave reproducible images.

Contact Angle Measurement

To characterize the coating, contact angles in deionized water were measured on flat plate and glass fiber samples using a dynamic contact angle analyzer (CAHN DCA 322 Cahn, Madison, WI, USA) at a platform speed of 80.0 μm/s. Ten coated fibers with average diameter of 15 μm were immersed at one time to improve the signal-to-noise ratio. The fibers were prepared for testing by placing two 2.54 cm pieces of double stick tape 2 cm apart on low-stick Nylon paper. Ten fibers were carefully extracted from the fiber tow and placed perpendicular to the two pieces of tape and parallel to each other. After placement of the 10 fibers, the double stick tape was covered on the exposed side with single-sided tape to hold the fibers in place. The mounted fibers were cut between the two pieces of tape, producing two test specimens with fibers 1 cm in length as shown below (Figure 1).

Each specimen was lifted from the low-stick nylon paper, exposing the underside. The underside was then covered with single-sided tape and the excess tape removed. Two sets or four samples were made for testing from each batch. The wetting experiment consists of moving a liquid surface up and down along the length of the fibers. A sample is fixed to a small metal hook and hung vertically from the measuring arm of the CAHN recording microbalance. The combined mass of hook and fibers is tared electronically. The wetting liquid is placed in a 100 ml beaker directly beneath the fibers. Fiber diameters are measured using an optical micrometer (VIA-100 from Boeckeler, Tucson, AZ, USA) attached to the video system. Surface tension measurements are obtained with a Wilhelmy plate. Four runs were measured for each test and the experimental scatter was approximately $\pm 2°$. Experimentally, two contact angles were measured for each sample: an advancing angle, as the liquid advances onto the fiber or glass plate, and a receding angle, as the liquid recedes from the fiber or glass plate.

FIGURE 1 A specimen showing fiber arrangement for contact angle measurement.

Fourier Transform Infrared Spectroscopy (FTIR) Analysis

Diffuse reflectance infrared Fourier transform (DRIFT) spectra of the coated and bare E-glass fibers were collected using a Magna-IR 550 (Magna, Madison, WI, USA) Fourier transform spectrometer equipped with a mercury-cadmium-telluride (MCT) detector (the standard instrument uncertainty in measuring wave number is $\pm 0.01\,cm^{-1}$, the cm^{-1} were rounded off to the nearest $1\,cm^{-1}$). Nitrogen was used as the purge gas. A Praying Mantis diffuse reflectance cell (DRA-100, Harrick Scientific Corporation, Ossining, NY, USA) having two hemispherical mirrors collected the diffuse reflectance spectra. Enough coated E-glass fibers and acetone-cleaned bare E-glass fibers were manually ground to fill the sample dish completely. The filled sample dish was covered by a smoothed-over layer of potassium bromide (KBr) powder (purchased from Aldrich Chemical Co. (Milwaukee, WI, USA) at purity of greater than 99%). Single beam reflectance data were ratioed against KBr, and the Kubelka-Munk function was plotted to obtain diffuse reflectance spectra at a resolution of $4\,cm^{-1}$. The reported spectra are signal averaged from 2000 scans between $4000\,cm^{-1}$ to $1200\,cm^{-1}$.

Ellipsometry

Ellipsometry provided a means of determining the film thickness on the substrate. All measurements were taken on a Discrete Polarization

Modulation Automatic Ellipsometer (INOMTECH, Inc., West Hartford, CT, USA) equipped with a He-Ne laser (632.8 nm) operated at an incident angle of 70°. All calculations were done with a two-layer step profile model assuming fixed refractive indices of 1.42 for the coupling agents on top of the native SiO_2 layer. According to Wassermann *et al.* [11], altering this value by 0.05 resulted in less than a 1 Å change in the calculated thickness of the coating. This refractive index (n) is approximately that of both liquid and solid straight-chain hydrocarbons ($n = 1.42$ to 1.44) [12]. The oxide thickness on the silicon wafer was measured for each sample and then subtracted from the total thickness of the oxide plus coupling agent layer to yield the deposited layer thickness. A three-phase model was used for thickness calculations along with a software program (COMPEL) developed by Inomtech Inc [13]. Five different spots on each sample were recorded.

Scanning Electron Microscopy

Scanning electron microscopy (SEM) was used to study the fracture surface of glass-fiber-reinforced epoxy composites. The fracture surface of the composite was gold-coated by a SEM coating system (Polaron, Agawam, MA, USA). A total gold film thickness of 200 Å was deposited on the fracture surfaces to avoid accumulation of electrical charge on the surface while performing SEM examination. A JEOL JSM-5300 SEM scanning microscope (Jeol, Peabody, MA, USA) was used to examine the fracture surfaces at 50× magnification.

RESULTS AND DISCUSSION

Ellipsometry

It is well known that hydrolysis of alkoxysilanes in an aqueous environment results in the formation of hydroxysilane compounds. To verify layer thickness, ellipsometry measurements were carried out, giving values of (19 ± 3) Å for all samples (where uncertainty is taken as one standard deviation). Table 1 summarizes the thickness data of pure and mixed coupling agents deposited on silicon wafer. It is not certain at this point why the aqueous deposition process produces multilayer films. Nucleophilic substitution of alkoxy groups by the amine group, which will connect the layers to form the multilayer, cannot be a plausible mechanism, because alkoxysilanes are resistant to nucleophilic attack of the primary amines [14]. It has been proposed that alkoxysilane and chlorosilane reagents hydrolyze first to form hydroxysilane compounds and then dehydrate to form siloxane bridges not only between the hydroxysilanes and the hydroxyl groups on the substrate [15, 16], but with each other. In this mechanism, the

TABLE 1 Thickness of Coupling Agent Layer on Silicon Wafers

Coupling agent concentration $(4.5 \times 10^{-3}\,\text{mol/L})$	Thickness of coupling agents coated on silicon wafers, Å*
PTMS (0 mol% amine)	20 ± 4
APS/PTMS (50 mol% amine)	18 ± 5
APS (100 mol% amine)	19 ± 4

*Number after $\pm$ is one standard deviation from the mean and is taken as the standard uncertainty.
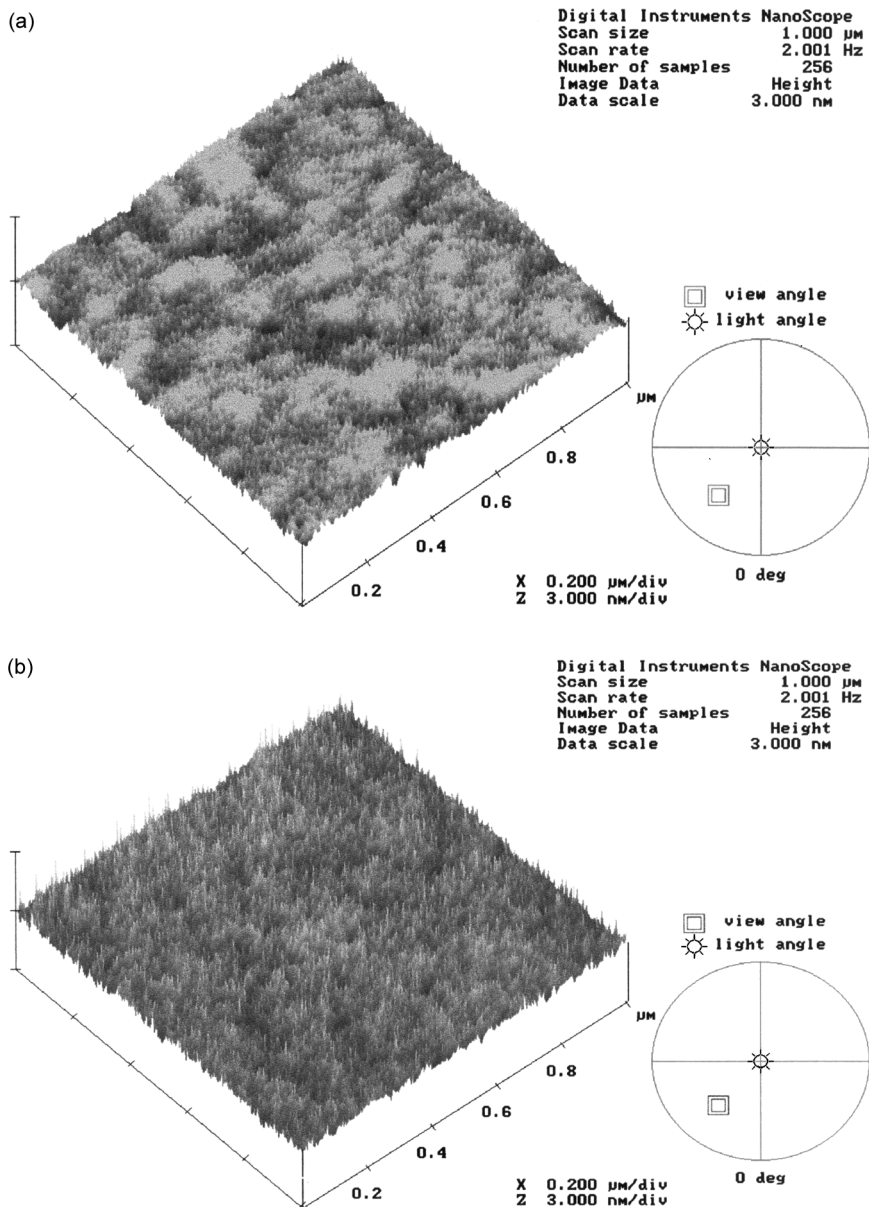
trialkoxysilane compound naturally has a higher chance of forming a three-dimensional network leading to the formation of thick films. The ellipsometry results indicate that the thickness of these pure and mixed deposited films, correspond to multilayer. The measured values support multilayer coverage. The ellipsometric data taken on the mixed films vary significantly from site to site, resulting in the large scatter observed in the thickness data. This suggests that the variation could result from uneven coverage or island formation of coupling agent on the substrate.
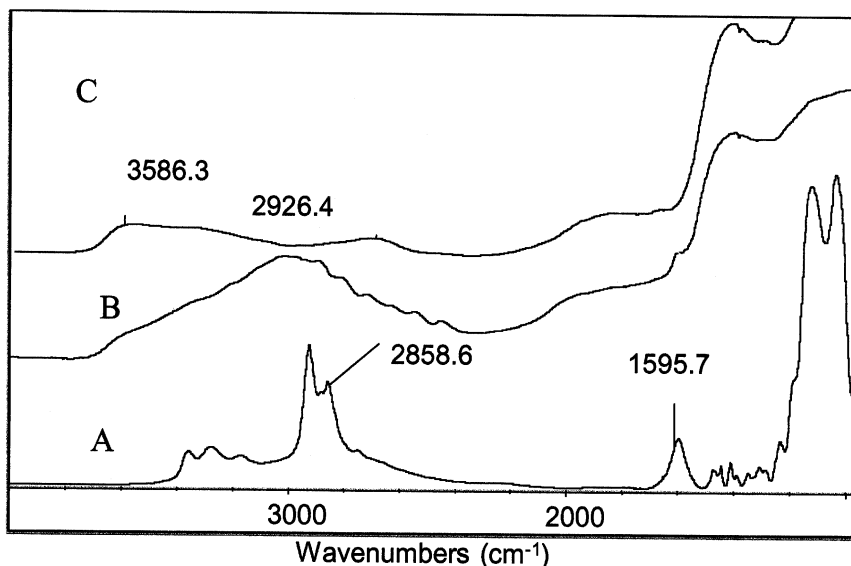
Microscopic Methods

Tapping mode atomic force microscopy (TMAFM) under ambient conditions was used to examine the morphology of a 50/50 mixture of APS/PTMS on silicon wafer. Figure 2a shows a three-dimensional topographic TMAFM image for a 50/50 mixture of APS and PTMS film on silicon wafer. There are islands of elevated regions surrounded by depressed regions. The formation of noncontinuous structures may be the result of phase separation of PTMS from APS in aqueous solution, caused by the difference in hydrophilicity of the molecules. Figure 2b shows a three-dimensional topographic TMAFM image for bare silicon wafer as a control specimen.

FTIR Characterization

IR spectroscopy has been commonly employed to characterize the silane coupling agent coating on inorganic oxides. Since it is difficult to analyze inorganic oxides on glass surfaces using transmission or attenuated total reflectance, a number of studies have relied on DRIFT (diffused reflectance infrared Fourier transform spectroscopy) to analyze E-glass surface coatings. The DRIFT spectra of the neat APS, E-glass fiber coated with $4.5 \times 10^{-2}\,\text{mol/L}$ APS and bare glass fiber in the region $4000-1200\,\text{cm}^{-1}$ are shown in Figure 3. Untreated E-glass
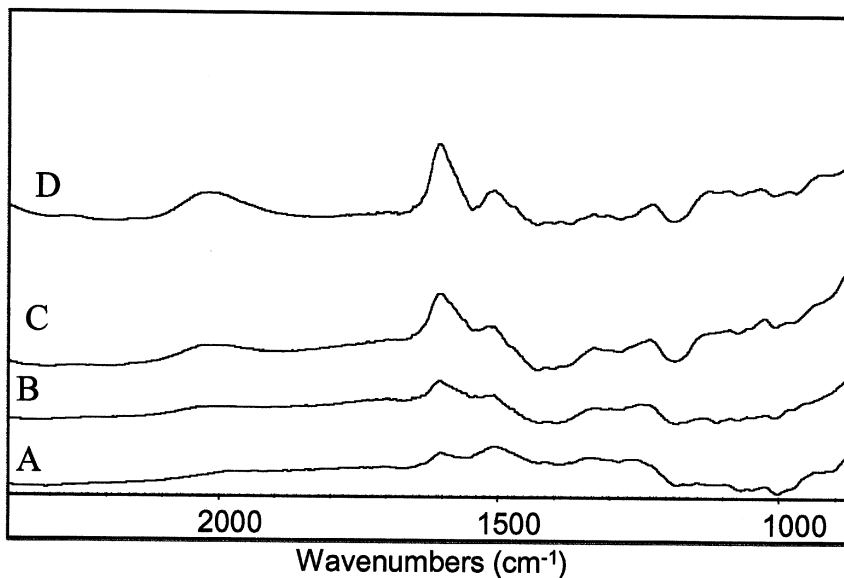
(a)

Digital Instruments NanoScope
Scan size   1.000 µM
Scan rate   2.001 Hz
Number of samples   256
Image Data   Height
Data scale   3.000 nM

view angle
light angle

µM

0.8

0.6

0.4

0.2

X 0.200 µM/div
Z 3.000 nM/div

0 deg

(b)

Digital Instruments NanoScope
Scan size   1.000 µM
Scan rate   2.001 Hz
Number of samples   256
Image Data   Height
Data scale   3.000 nM

view angle
light angle

µM

0.8

0.6

0.4

0.2

X 0.200 µM/div
Z 3.000 nM/div

0 deg

FIGURE 2 (a) TMAFM of APS/PTMS (50 mol% amine) film on silicon wafer; three-dimensional topographic image. (b) TMAFM of bare silicon wafer; three-dimensional topographic image (see Color Plate I).
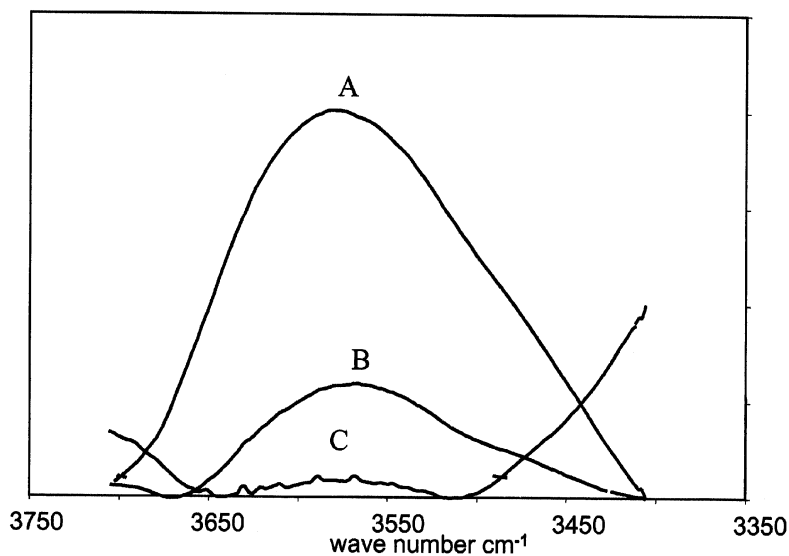
FIGURE 3 (a) DRIFT spectrum of neat APS; (b) DRIFT spectrum of APS $(4.5 \times 10^{-3} \, \text{mol/L})$ treated E-glass fiber with a KBr overlayer; (c) DRIFT spectrum of acetone-cleaned glass fiber with KBr overlayer.

fiber shows a broad Si-OH peak at $3590 \, \text{cm}^{-1}$ and the first overtone of the boron-oxygen stretching vibrations at $2680 \, \text{cm}^{-1}$. The neat APS displays methylene stretching modes of the propyl chain at $2926 \, \text{cm}^{-1}$ and $2858 \, \text{cm}^{-1}$. This spectrum also shows a distinct peak at $1595 \, \text{cm}^{-1}$ which can be assigned to the NH_2 deformation mode. In contrast, the condensed APS on E-glass fiber contains broad bands at $(3500 \text{ to } 2800) \, \text{cm}^{-1}$ and $(1600 \text{ to } 1300) \, \text{cm}^{-1}$. The broad band between $3500 \, \text{cm}^{-1}$ and $2800 \, \text{cm}^{-1}$ is due to CH_2 (stretching), NH_2 (stretching), and intermolecularly hydrogen-bonded Si-OH groups [17].

Figure 4 shows the DRIFT spectra with increasing concentration of silane solutions from $4.5 \times 10^{-3} \, \text{mol/L}$ to $4.5 \times 10^{-2} \, \text{mol/L}$ APS coated on glass fiber. The treated E-glass fiber DRIFT spectra are subtracted from the bare E-glass fiber spectrum to relate the intensity of the NH_2 peak at $1600 \, \text{cm}^{-1}$ to the solution concentration sorbed on the glass surface. The DRIFT spectrum of $4.5 \times 10^{-3} \, \text{mol/L}$ APS shows a minor band at $3550 \, \text{cm}^{-1}$ indicating the presence of free Si-OH peak (Figure 5) [17]. However, the absence of the peak at higher concentrations suggests complete coverage of the glass fiber surface at these higher concentrations.
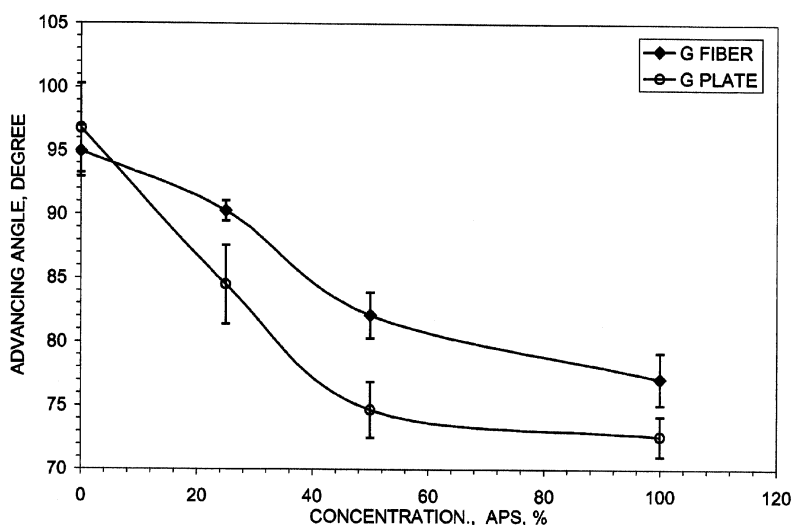
FIGURE 4 DRIFT spectrum of APS after subtraction of E-glass fiber, with increasing concentration APS (a) 4.5×10^{-3} mol/L, (b) 1.1×10^{-2} mol/L, (c) 2.2×10^{-2} mol/L, and (D) 4.5×10^{-2} mol/L.

FIGURE 5 Expanded view of APS-treated E-glass fiber from $3750-3400$ cm^{-1}, (a) bare glass fiber, (b) 4.5×10^{-3} mol/L, and (c) 4.5×10^{-2} mol/L.

Contact Angle Measurements

Depending on the selection of coupling agent, the coupling agent coated glass fiber can be involved in chemical bond formation with the polymer matrix. During deposition of coupling agent, the polar groups on the coupling agent can react with the hydroxyl groups present on the glass surface, as indicated by Ishida [5, 15]. Figure 6 shows the water contact angle of coupling agent coated on glass slides and glass fibers. As would be expected, the surface of PTMS coated fiber is very hydrophobic, while that of the APS coated fiber is less hydrophobic. For the mixed APS and PTMS coupling agents coated on glass surfaces, the contact angle measurements in water are intermediate between pure APS and pure PTMS. These data are in good agreement with the literature [18]. It appears from the results that increasing the portion of functional groups in solution increases the portion of functional (polar) groups on the surface. In fact, for pure APS deposited on glass fiber, a water contact angle of 73° indicates that the surface is more hydrophilic than pure PTMS deposited on glass surface. To address the question of bonding of coupling agent with the epoxy and the dependence of bonding on the concentration of amine groups in the mixture of the coupling agent mixture, SFFTs were performed.
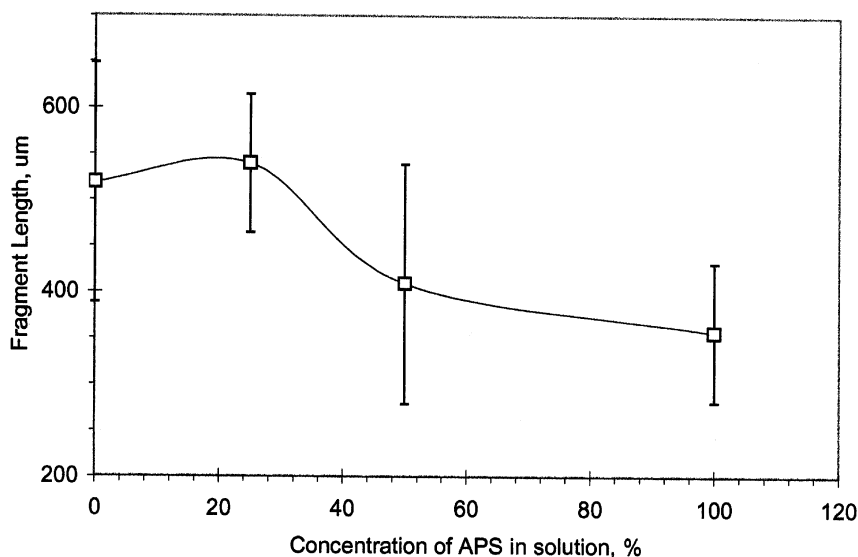

FIGURE 6 Contact angles for coatings of APS, and PTMS mixtures on glass fiber and glass plate (error bar represents one standard deviation from the mean and is taken as the standard uncertainty).
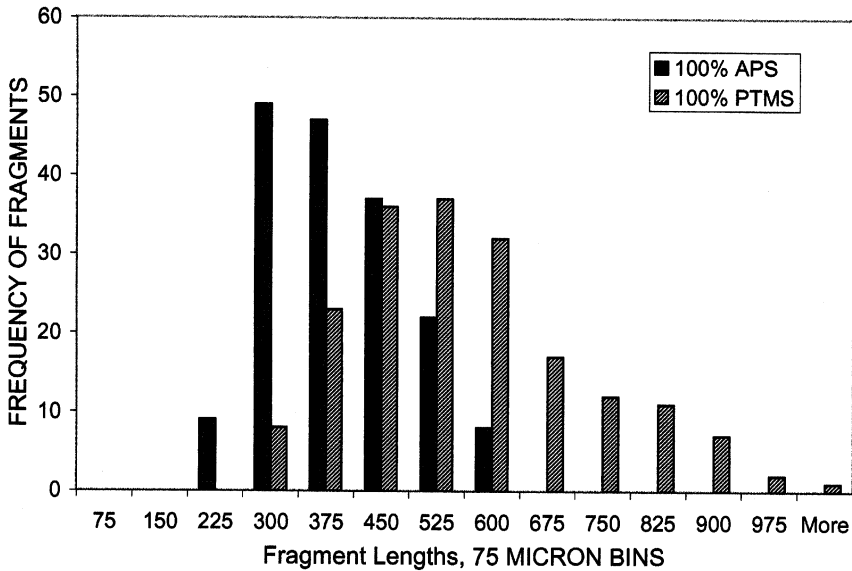
SFFTs Data Analysis

The bonding between the fiber and matrix for different coupling agent compositions has been quantitatively compared by measuring the average fragment length and determining the interfacial shear strength from SFFT data. The average fragment length is plotted as a function of coupling agent composition in the solution mixture in Figure 7. In this figure, the average fragment length decreases with increasing APS concentration. Since APS bonds covalently to the epoxy resin matrix during curing [19], this data indicates that covalent bonding increases fiber-matrix interfacial adhesion. This trend parallels the trend in the contact angle measurements performed in the previous section (see Figure 6), where the hydrophobic character of the deposited silane decreases with increasing APS concentration.

Figure 8 shows the E-glass fiber fragment length distribution (frequency) for APS and PTMS sized fiber composites at saturation. The fragment lengths were measured after relaxing the saturated SFFT specimen to the unstressed state. For the aggregated histogram of PTMS-coated specimens, the fragment length distribution at saturation exhibited a positive skewness (skewness/std. error $= 0.667/0.178 =$ 3.74). In contrast, the skewness ratio for the aggregated histogram of

FIGURE 7 Average fragment length for E-glass fibers coated with APS and PTMS mixture by aqueous deposition process (error bar represents one standard deviation from the mean and is taken as the standard uncertainty).
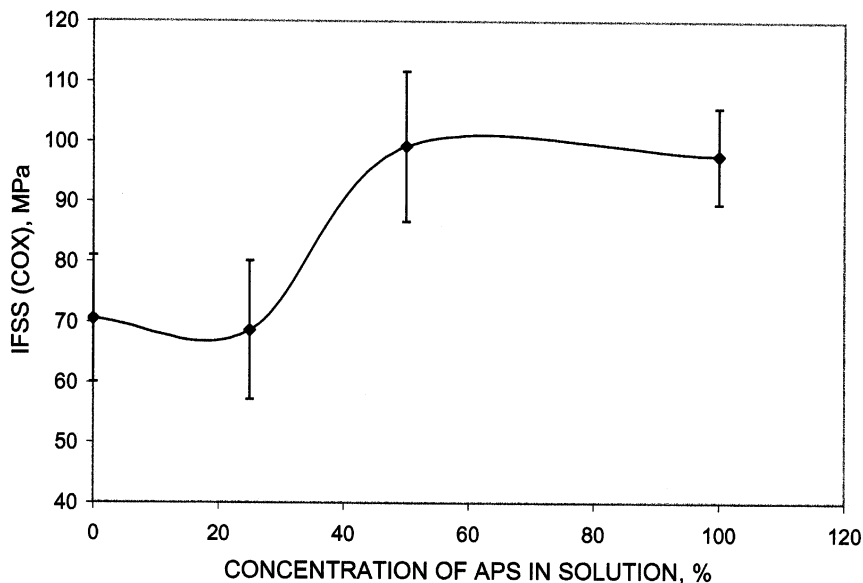
FIGURE 8 Average fragment length distribution at saturation for E-glass fibers deposited with APS and PTMS by aqueous deposition process.

APS-coated specimens was less (skewness/std. error $= 0.360/0.185 = 1.94$). Skewness characterizes the extent of asymmetry in a distribution around its mean by quantifying the degree to which the asymmetric tail extends toward more positive values.

The kurtosis ratio in the aggregated histogram of PTMS and APS specimens are -0.27 and -1.98, respectively. Kurtosis characterizes the relative peakedness or flatness of a distribution compared with the normal distribution. Negative kurtosis indicates a relatively flat distribution. Normality of the distribution is typically rejected if the ratio of either statistic to its standard error is less than -2 or greater than $+2$ [20]. Therefore, 100 mol% APS-treated specimens yield fragment distributions within the limits of normality, whereas the fragment distributions from 100 mol% PTMS-treated specimens exhibit positive skewness. These results show an effect similar to Holmes et al. [8] in their previous work on the effect of strain rate on interfacial shear strength measurements.

Figure 9 shows the result for IFSS as a function of coupling agent composition in the mixture. The IFSS between the epoxy matrix and E-glass fibers treated with mixed APS and PTMS appears to increase sharply as the composition of APS component in the mixture increases from (25 to 50) mol% APS.

FIGURE 9 Average IFSS for E-glass fibers coated with APS and PTMS mixtures by aqueous deposition process (error bar represents one standard deviation from the mean and is taken as the standard uncertainty).

To examine whether this sharp increase in the IFSS with coupling agent composition is statistically significant, analysis of variance (ANOVA) was used. In this analysis, confidence levels below 95% are treated as equivalent (i.e., no statistically significant difference). Single factor ANOVA statistics indicate that the IFSS for a 100 mol% APS specimen is distinguishable at the 95% confidence level (p value [21] < 0.05) from the IFSS value for a 100 mol% PTMS specimen (p value $= 0.005$). Therefore, ANOVA indicates that the type of coupling agent (*i.e.*, bonding versus nonbonding) does have a significant role to play in IFSS.

However, there is no significant difference in the IFSS value between 100 mol% PTMS and 25 mol% APS (p value $= 0.925$), and between 50 mol% APS and 100 mol% APS (p value $= 0.369$). In contrast, there are significant differences in the IFSS value between 25 mol% APS and 50 mol% APS at the 95% confidence level (p value $= 0.02$). This indicates that the increase in IFSS with increased bonding sites is nonlinear and follows an S-shaped curve.

Of particular interest on the S-shaped curve in Figure 9 is the average IFSS of (74.5 ± 2.6) MPa for the nonbonding PTMS, where
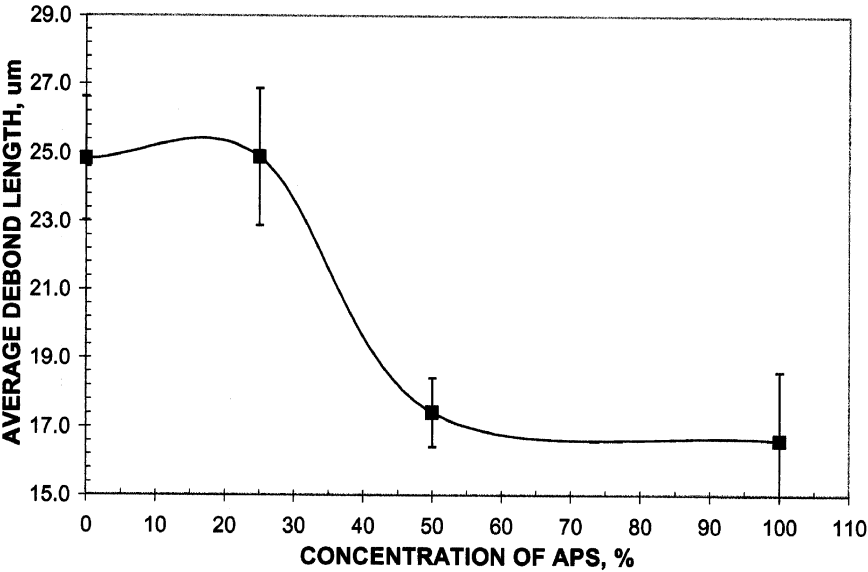
the coupling agent is not covalently bonded to the epoxy matrix. These results parallel previously reported data by Hunston et al. [7], where n-octadecyl trichlorosilane was used for the nonbonding silane coupling agent. Interestingly, dynamic contact angle measurements of the fiber surfaces coated with 100% nonbonding silane coupling agent indicated complete hydrophobic character. Despite the absence of covalent bonding, the IFSS value of (74.5 ± 2.6) MPa indicates that there is actually a significant interaction between the matrix and fiber.

Sharpe [22] and Drzal [23] have ascribed adhesion at the fiber-matrix interface of composites to the following factors: (1) mechanical interlocking, (2) physicochemical interactions, (3) chemical interaction, and (4) mechanical deformation of the fiber-matrix interphase region. The magnitude of fiber-matrix adhesion was quantified mathematically as the sum of the first three factors by Nardin and Ward [24]. Since the deformation rate is the same for all samples and covalent bonding is "formally" eliminated because of the absence of functional groups on the 100 mol% PTMS silane coupling agent layers, fiber-matrix adhesion in the 100 mol% PTMS interface is attributed to mechanical interlocking and physicochemical interactions.
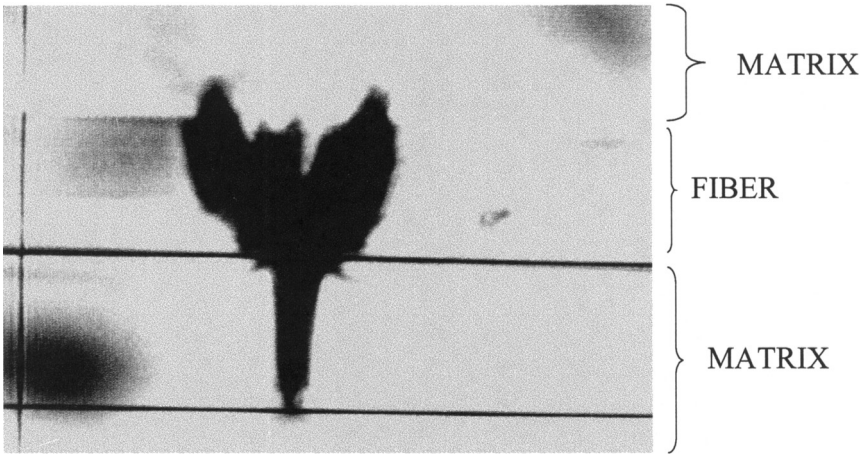
Parallel research by the authors of this paper [25] showed that the level of adhesion observed with the solvent-deposited nonbonding propyltrichloro silane (PTCS) interface is due primarily to mechanical interlocking, with a small contribution arising from physicochemical interactions. For the 100% bonding aminopropyltrichloro silane (APTCS) (IFSS $= (98 \pm 10)$ MPa) silane deposited on E-glass fibers under solvent conditions the IFSS increased by an additional 31% relative to the nonbonding solvent interface. This research indicates that the level of adhesion observed with the 100% APS silane coupling agent interface is enhanced by the amine group on E-glass fiber surface.

This improved adhesion was observed by Ahagon and Gent [6], who showed that when glass plates are treated with vinyl and ethyl silane coupling agent, the strength of adhesion between glass plates and polybutadiene elastomer increased as the composition of the vinyl coupling agent in the coupling agent mixture increased. The non-bonding component is ethyl silane and the bonding component is vinyl silane. The bonding component reacts with the unsaturated poly-butadiene, to form a covalent link.
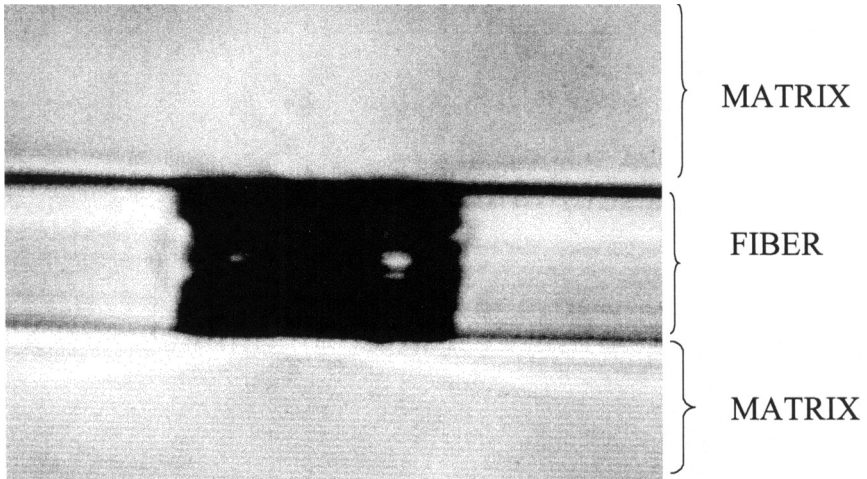
The failure mode of a composite at the fiber-matrix interface can be characterized by studying the debond region of fibrous composite after fiber fracture. A plot of debond length as a function of increasing concentration of APS is shown in Figure 10. The justification for
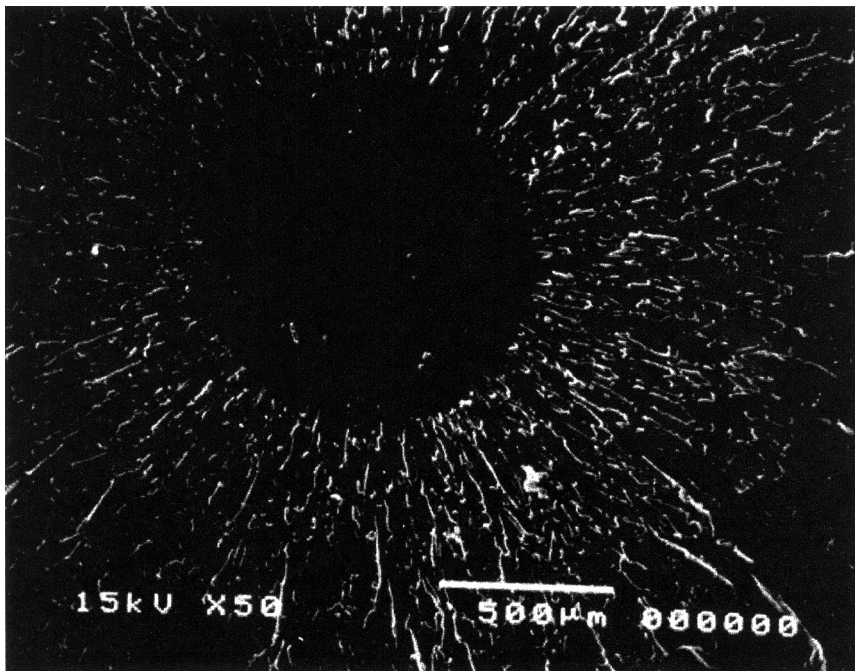
FIGURE 10 Average debond length for E-glass fibers coated with APS and PTMS mixture by aqueous deposition process (error bar represents one standard deviation from the mean and is taken as the standard uncertainty).
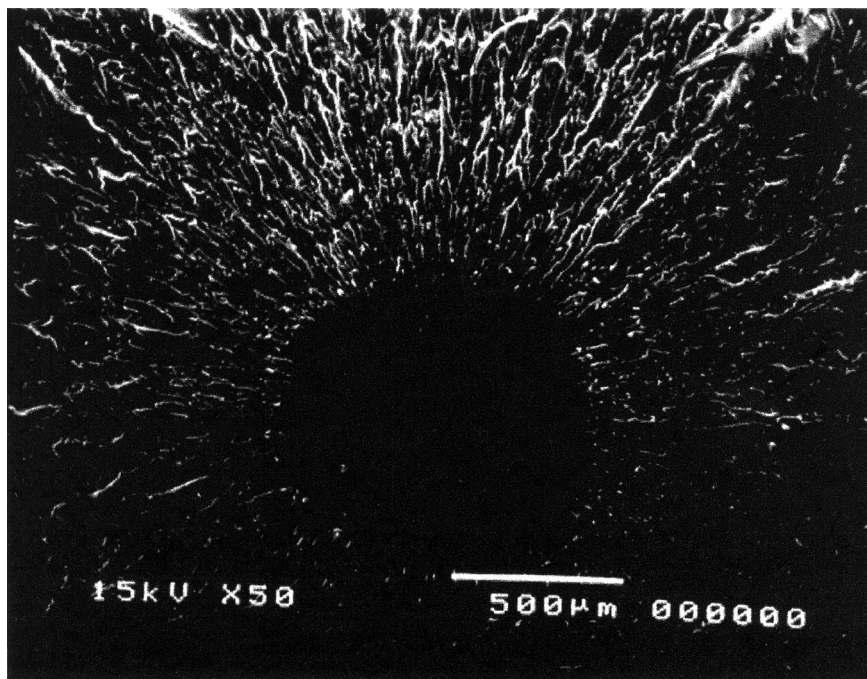

FIGURE 11 The darkened regions associated with the fiber breaks in APS-coated glass fiber epoxy composite.

FIGURE 12 Darkened regions associated with the fiber breaks in PTMS-coated glass fiber epoxy composite.
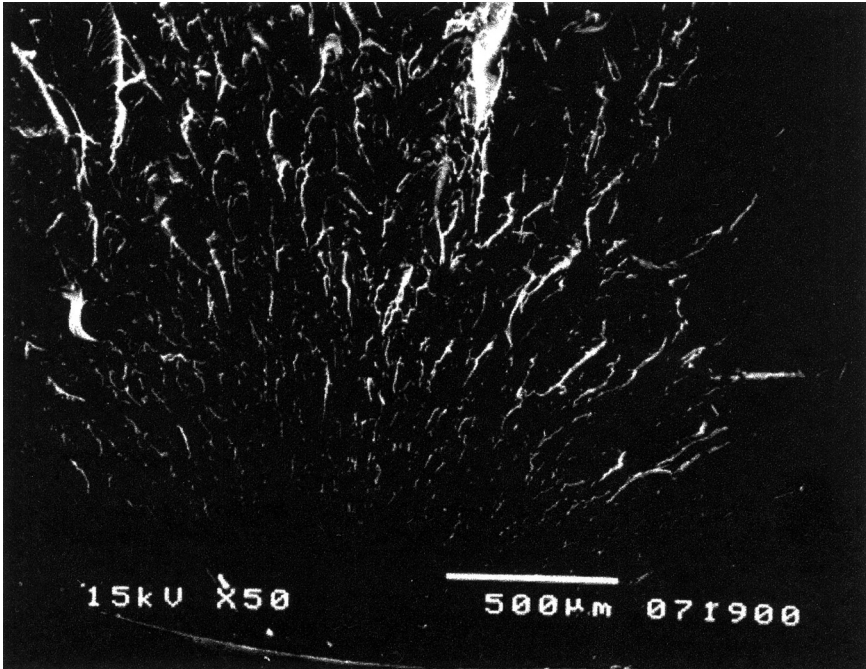

FIGURE 13 SEM micrographs of the fracture surface of APS-coated glass fiber epoxy composite.

FIGURE 14 SEM micrographs of the fracture surface of APS/PTMS-coated glass fiber epoxy composite.

delineating these darkened regions as consisting of matrix material debonded from the fiber is reported elsewhere [26]. The debond length was found to decrease as a function of increasing concentration of APS in the coupling agent mixture. To understand the debonding failure mechanism in the composite, the regions associated with the fiber breaks in coupling agent-coated E-glass fiber/epoxy composite were carefully analyzed. Figures 11 and 12 show the darkened regions associated with the fiber breaks in APS and PTMS coated system, respectively. In Figure 11, a matrix crack is formed perpendicular to the fiber axis, in addition to fiber-matrix debond region when the fiber fractures. In Figure 12, the energy generated by the fracture of the glass fiber is absorbed by fiber-matrix debonding (i.e., no matrix crack formation).

In this study, the bonding between fiber and matrix for different coupling agent compositions has been qualitatively compared by characterizing the mirror zone of the fractured surface of the glass fiber epoxy composite. The work of Drzal et al. [27] has shown that the

FIGURE 15 SEM micrographs of the fracture surface of PTMS-coated glass fiber epoxy composite.

size of the mirror zone depends on the brittleness/ductility of the material. Consistent with Drzal's results the 100 mol% APS interface yields a larger mirror zone than the 50 mol% APS interface (see Figures 13 and 14). For nonbonding coupling agent PTMS, the mirror zone is the smallest at the interface region, and it is noticed at the edge of the composite (Figure 15). These results qualitatively indicate that the degree of bonding may have a profound influence on the failure mode of fiber-matrix interface during fiber fracture.

CONCLUSIONS

The following conclusions can be drawn from our work:

1. TMAFM and Ellipsometry were used to characterize the morphology and thickness of coupling agent mixtures deposited on the silicon wafers, respectively, and we found that the thickness of the deposited films correspond to multilayers.

2. Using DRIFT analysis we found that E-glass fibers are partially covered at coupling agent concentrations lower than 4.5×10^{-2} mol/L.
3. Contact angle measurements show an increase in the polarity of glass surface as the APS component in the mixture is increased.
4. SFFT results indicate that the IFSS increases as the composition of the bonding coupling agent increases in the solution mixture. For 100% APS-coated glass fiber epoxy composite, matrix cracks were found to be formed in addition to fiber-matrix debonding.
5. The type of coupling agent and the composition of coupling agent mixture have been shown to influence the adhesion between glass fiber and epoxy matrix.

REFERENCES

[1] Moussawi, H. A., Drown, E. K., and Drzal, L. T., *Polym. Composites*, **14**, 195–200 (1993).
[2] Koenig, J. L., "FTIR Studies of Interfaces." In: *Silanes, Surfaces and Interfaces*, Leyden, D. E., Ed. (Gordon & Breach Science Publishers, New York, 1986), pp. 43–57.
[3] Wu, H. F., Dwight, D. W., and Huff, N. T., *Composite Sci.*, **57**, 975–983 (1997).
[4] Nishioka, G. M., *J. Non-Cryst. Solids*, **120**, 102–107 (1990).
[5] Ishida, H., and Suzuki, Y., *Composite Interfaces*, **14**, 317–327 (1986).
[6] Ahagon, A., and Gent, A., *J. Polym. Sci.*, **13**, 1285–1300 (1975).
[7] Hunston, D. L., Macturk, K., Schultheisz, C., Holmes, G., McDonough, W., and Schutte, C., *Proc. EURAD '96, European Adhesion Conf.*, Cambridge, England, Sept. (1996), pp. 1–5.
[8] Holmes, G. A., Peterson, R. C., Hunston, D. L., McDonough, W. G., and Schutte, C. L., "The Effect of Nonlinear Viscoelasticity on Interfacial Shear Strength Measurements." In: *Time Dependent and Nonlinear Effects in Polymers and Composites*, R. A. Schapery, Ed. (ASTM, **STP 1357**, 2000) West Conshocken, PA, pp. 98–117.
[9] Based on report provided by Evans East, (Gaithersburg, MD, 1996) and contracted by NIST.
[10] Drzal, L. T., and Herrera-Franco, L. P. J., "Composite Fiber-Matrix Bond Test." In: *Engineered Materials Handbook: Adhesives and Sealants* (ASM International, Metals Park, OH, 1990), pp. 392–405.
[11] Wassermann, S. R., Tao, Y. T., and Whitesides, G. M., *Langmuir*, **5**, 1074–1087 (1989).
[12] Weast, R. C., *CRC Handbook of Chemistry and Physics* (CRC Press, Inc., Cleveland, OH, 1975).
[13] (Inomtech Inc., West Hartford, CT).
[14] Corriu, R. J. P., and Guerin, C., *Adv. Organmet. Chem.*, **20**, 265–268 (1982).
[15] Plueddemann, E. P., *Silane Coupling Agents* (Plenum Press, New York, 1991).
[16] Ulman, A., *Chem. Rev.*, **96**, 1533–1554 (1996).
[17] Culler, S. R., Ishida, H., and Koenig, J. L., *Appl. Spectroscopy*, **38**(1), 1–7 (1984).
[18] Holmes, G. A., Cheng, J. F., Wu, B., Mao, G., and Peterson, R. C., *Proc. 13th Annual Technical Conference on Composite Materials* (Baltimore, Maryland, 1998), pp. 400–415.

[19] Wang, D., and Jones, F. R., *Composite Science and Technology*, **50**, 215−228 (1994).

[20] SPSS Base 8.0 Applications Guide (SPSS Inc., Chicago, 1998), pp. 27−28.

[21] Ott, R. L., *An Introduction to Statistical Methods and Data Analysis* (Duxibury Press, Belmont, CA, 1993), pp. 230−237.

[22] Sharpe, L. H., *J. Adhesion*, **4**, 51−64 (1972).

[23] Drzal, L. T., "Fiber-Matrix Interphase Structure and Its Effect on Adhesion and Composite Mechanical Properties." In: *Controlled Interphases in Composite Materials*, H. Ishida, Ed. (Elsevier Press, New York, 1990), pp. 309−320.

[24] Nardin, M., and Ward, I. M., *Materials Science and Technology*, **3**, 814−819 (1987).

[25] Holmes, G. A., Feresenbet, E., and Raghavan, D., *Composite Interfaces*, accepted.

[26] Holmes, G., Peterson, R. C., Hunston, D. L., and McDonough, W. G., *Polym. Composites*, **21**(3), 450−465 (2000).

[27] Al-Moussawi, H., Drown, E. K., and Drzal, L. T., *Polym. Composites*, **14**(3), 195−200 (1993).